DALTON
FULL PAPER

Coligand tuning of the DNA binding properties of bioorganometallic (η^6-arene)ruthenium(II) complexes of the type [(η^6-arene)Ru(amino acid)(dppz)]$^{n+}$ (dppz = dipyrido[3,2-*a*:2′,3′-*c*]phenazine), *n* = 1–3

André Frodl, Diran Herebian and William S. Sheldrick *

Lehrstuhl für Analytische Chemie, Ruhr-Universität Bochum, D-44780 Bochum, Germany.
E-mail: shel@anachem.ruhr-uni-bochum.de

Received 11th April 2002, Accepted 23rd July 2002
First published as an Advance Article on the web 3rd September 2002

The DNA binding of cationic complexes of the type [(η^6-arene)Ru(Aa)(dppz)] $(CF_3SO_3)_n$ (arene = C_6H_6, $Me_3C_6H_3$, C_6Me_6; dppz = dipyrido[3,2-*a*:2′,3′-*c*]phenazine; *n* = 1, Aa = AcH_{-1}cysOH **4**–**6**; *n* = 2, Aa = AcmetOH **7**–**9**; *n* = 3, Aa = H_2metOMe **10**–**12**) containing S-coordinated amino acids (HcysOH = L-cysteine, HmetOH = L-methionine) has been studied by UV-vis titration and 2D-NOESY. Stable intercalative binding is indicated for these complexes by their steady decrease in absorbance at maxima between 350 and 390 nm on titration with CT DNA and the bathochromic shifts of these absorption maxima. Taking **4**–**12** and the analogous (η^6-C_6Me_6)Ru^{II} complexes of the tripeptides HglyglycysOH (*n* =1, **13**) and HglyglymetOH (*n* = 2, **15**; HglyOH = glycine) into account, typical DNA binding constant (K_b) ranges can be established for (η^6-arene)Ru^{II} complexes: 5.3×10^4–1.6×10^5 M^{-1} for monocations, 6.3×10^5–9.9×10^5 M^{-1} for dications and 1.6×10^6–5.5×10^6 M^{-1} for trications. These K_b values clearly reflect a strengthening of electrostatic interactions with the negatively charged phosphodiester backbone of DNA as the total cation charge increases. A consistent trend to higher K_b values is also apparent for the coligand series C_6H_6 < $Me_3C_6H_3$ < C_6Me_6 with the relative increase being, in general, more pronounced for C_6H_6/$Me_3C_6H_3$ pairs. The strong electronic influence of the coligand on dppz intercalation is also reflected by marked increases ΔT_m of 18.2–18.5 °C in the CT DNA thermal denaturation temperature for di- and tri-cationic (η^6-C_6Me_6)Ru^{II} complexes. Upfield ^{1}H NMR chemical shifts and characteristic NOE cross peaks for the dppz protons of the 1 : 1 complex formed between **9** and $d(GTCGAC)_2$ are consistent with a side-on intercalation adjacent to T_2 from the major groove.

Introduction

In contrast to the extensive studies[1,2] on transition metal polypyridyl complexes such as $[Ru(bpy)_2(dppz)]^{2+}$, $[Ru(phen)_2(dppz)]^{2+}$ (bpy = 2,2-bipyridine, phen = 1,10-phenanthroline, dppz = dipyrido[3,2-*a*:2′,3′-*c*]phenazine)[3,4] and $[Rh(phen)_2(phi)]^{3+}$ (phi = 9,10-phenanthrene-quinone diimine),[5] only two reports on the intercalation of comparable organometallic complexes into DNA have appeared.[6,7] Hubbard *et al.*[6] provided gel electrophoretic evidence for an intercalative binding mode of $[(\eta^5\text{-}C_5Me_5)Ru(dppz)(NO)](OTf)_2$ into supercoiled plasmid DNA and we have investigated[7] the analogous interaction of half-sandwich complexes of the type $[(\eta^5\text{-}C_5Me_5)M(Aa)(dppz)]^{n+}$ (M = Ir, Rh; Aa = amino acid or peptide; *n* = 1–3) with calf thymus DNA (CT DNA) and plasmid *pBluescript II Ks+* (2958bp, 50.2% GC base pairs). The observed steady decrease in absorbance at maxima between 350 and 400 nm on UV-vis titration of such bioorganometallic compounds with CT DNA and the bathochromic shifts of these absorption maxima are consistent with stable intercalative DNA binding. However, the magnitudes of the total binding constants K_b (8.80×10^4–2.62×10^6 M^{-1}) are clearly dependent on the overall cation charge *n* (1–3), *i.e.* on additional electrostatic interactions with the negatively charged phosphodiester backbone of DNA.

This finding is in accordance with the results of Sartorius and Schneider[8] for intercalation studies on naphthalene, quinoline and indole derivatives with positively charged ammonium groups in their side chains. These authors also found that for the heterocyclic compounds studied, intercalation strength is essentially a function of the size of the aromatic system, independent of heteroatoms or the presence of local positive charges within such moieties. However, *ab initio* molecular orbital calculations[9,10] do stress the importance of corresponding neighbouring charge distributions for π-stacking of heteroaromatic ring systems such as nucleobases. One promising strategy for investigating the influence of such an electron correlation on metal complex/DNA interaction is to vary the ancillary ligands whilst retaining the original intercalating ligand (*e.g.* dppz). Unfortunately, the interpretation of such binding studies has often been hampered by the unavoidable introduction of additional competing interactions, *e.g.* hydrogen bonding or hydrophobic contacts. For instance, whereas the intercalating bimetallic ammine complex $[\{Ru(NH_3)_4\}_2(dpb)]^{4+}$ (dpb = 2,3-bis(2-pyridyl)-benzo[*g*]-quinoxaline) binds much more strongly to DNA[11] than the corresponding bpy complex $[\{Ru(bpy)_2\}_2(dpb)]^{4+}$, the presence of four NH_3 ligands is detrimental to DNA binding[12] for $[Ru(NH_3)_4(dppz)]^{2+}$ in comparison to $[Ru(phen)_2(dppz)]^{2+}$. Hydrogen bonding interactions were invoked as a possible explanation in both cases, as they were to explain the striking increase in the duplex melting temperature, ΔT_m, for $[Rh(phen)(phi)_2]^{3+}$ with a 15-mer (21 °C) in comparison to that for $[Rh(phen)_2(phi)]^{3+}$ (7 °C).[13]

We now report a comparative binding study of complexes of the type $[(\eta^6\text{-arene})Ru(Aa)(dppz)]^{n+}$ (*n* = 1–3), with methionine-(met) or cysteine-containing (cys) amino acids and peptides, in which the aromatic coligand (arene = C_6H_6, 1,3,5-$Me_3C_6H_3$, C_6Me_6, *p*-cymene) was varied so as to systematically influence the charge distribution within the dppz moiety. Apart from possible changes in the electron correlation between intercalating dppz ligands and the DNA nucleobases, only steric bulkiness and weak hydrophobic contacts can be directly affected by this coligand variation.

 DOI: 10.1039/b203569n

Results and discussion

The parent (η^6-arene)Ru^{II} complexes, [(η^6-arene)RuCl(dppz)]Cl **1**–**3**, (arene = C_6H_6, 1,3,5-$Me_3C_6H_3$, C_6Me_6), were prepared by reaction of the respective starting compounds [{(η^6-arene)-RuCl}$_2$(μ-Cl)$_2$] with dppz in ethanol. Fig. 1 depicts the X-ray

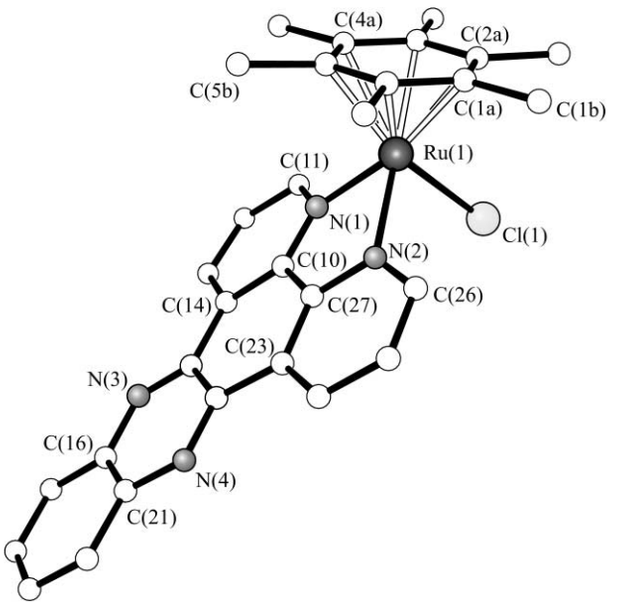

Fig. 1 Molecular structure of the cation of [(η^6-C_6Me_6)RuCl(dppz)]-(CF_3SO_3) **3b**. Selected bond lengths (Å): Ru(1)–Cl(1) 2.409(2), Ru(1)–N(1) 2.111(2), Ru(1)–N(2) 2.106(3).

structure of the monocation of **3b**, [η^6-C_6Me_6)RuCl(dppz)]-(CF_3SO_3), in which the Ru atom is sited 1.705(1) Å from the centroid of the η^6-coordinated C_6Me_6 moiety and this and the dppz ligand exhibit an interplanar angle of 50.7°. Ru–C distances fall in the narrow range 2.195(6)–2.203(9) Å. As to be expected, neighbouring dppz ligands participate in π-stacking in the monoclinic crystal lattice of **3b**. The effect of coligand variation on the electron distribution within the dppz aromatic system can be gauged by comparing the ^{1}H NMR shifts for individual protons, which were assigned on the basis of 2D experiments (H, H–COSY, HMQC–TOCSY, HMBC). With the exception of the H3, H8 resonances, all ^{1}H NMR signals in the dppz region shift systematically to higher field on going from **1** to **3** (Fig. 2). This increase in shielding is indicative of a weakening of the Ru–N(dppz) bonds within this series as a result of the concomitant increase in Ru–arene bond strength for the corresponding coligand in the order benzene < mesitylene < hexamethylbenzene. Whereas very pronounced upfield shifts are observed in **2** and **3** for the H2, H9 protons (respectively −0.19, −0.56 ppm) adjacent to the coordinating nitrogen atoms, those of H4, H7 (−0.06, −0.23 ppm), H11, H14 (−0.03, −0.19 ppm) and H12, H13 (−0.02, −0.10 ppm) are more modest and decrease with increasing remoteness from N1 and N10. Marginal lowfield displacements of respectively 0.01 and 0.03 ppm are apparent for the H3, H8 protons.

Mono-, di- and tri-cationic bioorganometallic complexes containing the aromatic coligands C_6H_6, 1,3,5-$Me_3C_6H_3$ and C_6Me_6 and respectively AcH_{-1}cysOH (**4**–**6**), AcmetOH (**7**–**9**) or H_2metOMe (**10**–**12**) were obtained by treating the solvent complexes [(η^6-arene)Ru(acetone)(dppz)](CF_3SO_3)$_2$ **1a**–**3a** with equivalent quantities of the individual amino acid. A CH_3OH–CH_2Cl_2 solvent mixture at 45 °C was employed for the preparation of **4**–**6**, acetone at 60 °C for the met-containing compounds **7**–**12**. The (η^6-C_6Me_6)Ru^{II} complexes [(η^6-C_6Me_6)-Ru(HglyglyH$_{-1}$cysOH)(dppz)](CF_3SO_3) (**13**), [(η^6-C_6Me_6)Ru-(HcysOMe)(dppz)](CF_3SO_3)$_2$ (**14**) and [(η^6-C_6Me_6)Ru(Hglyglymet OH)(dppz)](CF_3SO_3)$_2$ (**15**) were synthesised in an

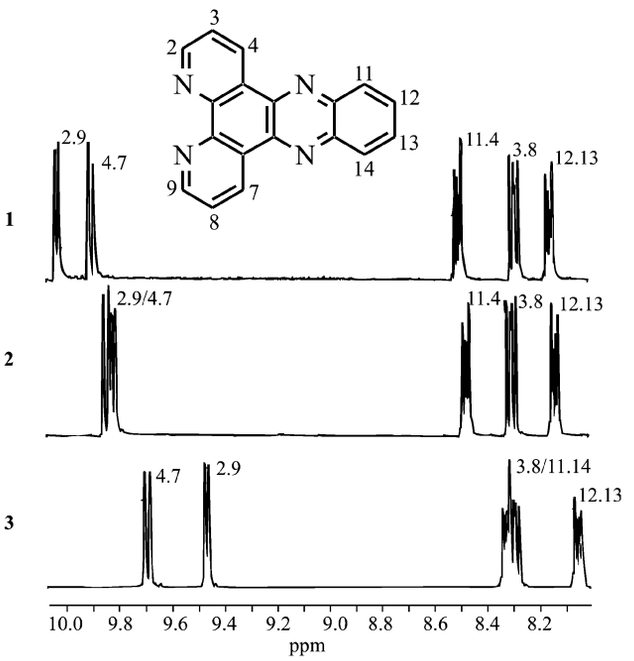

Fig. 2 A comparison of the dppz region of the ^{1}H NMR spectra of [(η^6-arene)RuCl(dppz)]Cl **1**–**3** (arene = C_6H_6, 1,3,5-$Me_3C_6H_3$, C_6Me_6) taken in CD_3OD.

analogous manner, either in water at 50 °C (**13**, **15**) or in a CH_3OH–CH_2Cl_2 mixture at 45 °C (**14**). Stirring of two equivalents of $Ag(CF_3SO_3)$ with acetone solutions of **1**–**3** for 30 minutes, followed by filtration of precipitated AgCl and solvent removal, afforded the acetone complexes **1a**–**3a** as viscous oils, which were employed without further characterisation.

The complexes **4**–**15** (Scheme 1) were characterised by FAB

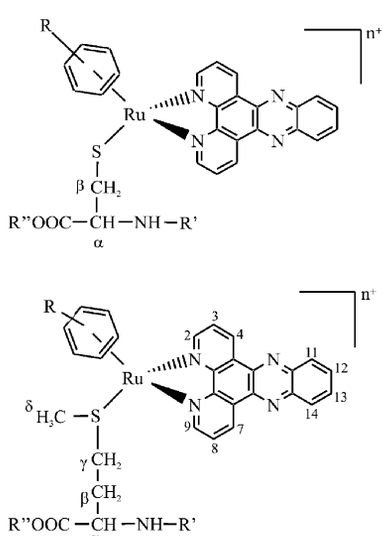

a) R'=Ac; Hglygly; R"=H
b) R'=H; R"=Me

Scheme 1 Structures of **4**–**15**.

mass spectrometry, ^{1}H and ^{13}C NMR and IR spectroscopy. A striking coligand upfield shift dependence in the order C_6H_6 < 1,3,5-$Me_3C_6H_3$ < C_6Me_6 is apparent not only for the dppz proton resonances, with the exception of H3, H8 as in **1**–**3**, but also for the amino acid ^{1}H NMR signals. For instance, the methionine δ-CH_3 ^{1}H NMR singlet in CD_3OD shifts from δ 2.12 over 1.78 to 1.65 in the AcmetOH series **7**–**9** and from δ 2.06 over 1.72 to 1.67 in the [H_2metOMe]$^+$ series **10**–**12**. Analogous upfield ^{13}C signal shifts are observed for the parent side chain methyl carbon atom in these complexes, namely δ 20.5, 18.6 and 16.7 for **7**–**9** and δ 19.9, 17.7 and 16.4 for **10**–**12**. Even more

pronounced spectral displacements are apparent for the β-CH_2 protons of the κ*S* coordinated AcH_{-1}cysOH complexes **4**–**6**, whose multiplets exhibit respective δ values of 2.5–2.8, 1.8/2.1 and 1.2–1.4. The apposite ^{13}C NMR shifts for the parent carbon atom are δ 36.4, 35.5 and 27.8 in CD_3OD. The magnetic resonance behaviour of the methionine δ-CH_3 protons in these bioorganometallic compounds represents a striking reversal in the characteristic positive shifts (from the δ value in free methionine of *ca*. 2.05–2.10) experienced by the same protons in $(\eta^6\text{-}C_6H_6)Ru^{II}$ and $(\eta^5\text{-}C_5Me_5)Ru^{II}$ complexes[14–16] without an additional chelating dppz ligand. Analogous negative shifts were also observed for the δ-CH_3 protons in half-sandwich complexes[7] of the type $[(\eta^5\text{-}C_5Me_5)Ir(Aa)(dppz)](CF_3SO_3)_n$ (Aa = AcmetOMe, $[H_2metOMe]^+$, HglyglymetOH).

Before turning to discussion of the DNA binding studies, it is necessary to consider the possible competition between intercalation and direct coordination by nucleobase nitrogen atoms for this class of bioorganometallic complexes. The kinetics of AcmetOH substitution by the model purine base 9-ethylguanine (9-Etgua) were, therefore, studied by ^1H NMR spectroscopy at pH 7.2 for complexes **7**–**9** (Fig. 3). The rate

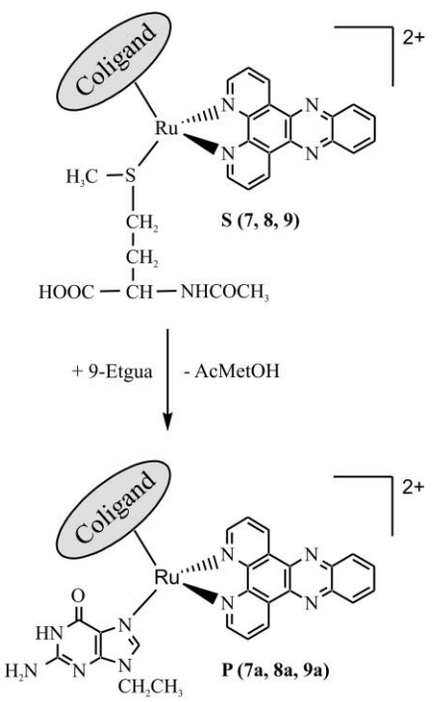

Fig. 3 Substitution of AcmetOH in complexes **7**–**9** (coligand = C_6H_6, $Me_3C_6H_3$, C_6Me_6) by 9-ethylguanine (9-Etgua).

of reaction was monitored by following the development of the integral value for the δ-CH_3 resonance of coordinated AcmetOH in **7**–**9** (c_t(S)) after a time span *t* in comparison to the sum of the integral values for δ-CH_3 (c_0(S)) in both these starting compounds and in the liberated amino acid at 2.07 ppm. After 90 hours a $c_t(S)/c_0(S)$ ratio of *ca*. 0.5 is observed for the hexamethylbenzene complex **9**. The ligand substitution involves initial slow dissociative loss of AcmetOH followed by rapid coordination of the $(\eta^6\text{-arene})Ru^{II}$ fragment by N7 of 9-Etgua. Linear regression analyses of the time-dependence of the function $\ln[c_t(S)/c_0(S)]$ (Fig. 4) provide respective rate constants *k* of $9.56(41) \times 10^{-7}$, $1.71(5) \times 10^{-6}$ and $2.39(10) \times 10^{-6}$ s^{-1} for the first order initial dissociative step in complexes **7**–**9**. Steadily increasing lability of the Ru–S(thioether) bond within this series clearly correlates with the strengthening of the Ru–coligand bonds in the order $C_6H_6 < Me_3C_6H_3 < Me_6C_6$. However, in accordance with previous comparative kinetic studies[17,18] on $(\eta^6\text{-arene})Ru^{II}$ and $(\eta^5\text{-}C_5Me_5)Ir^{III}$ half-sandwich complexes, the rate of reaction for **7**–**9** is much slower than for

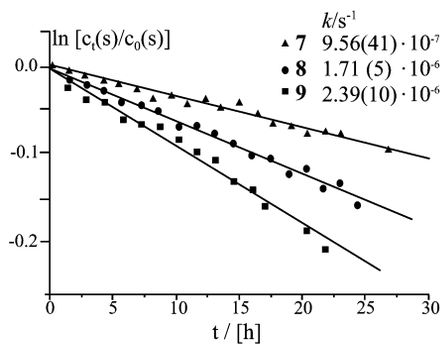

Fig. 4 Time-dependence of the ^1H NMR function $\ln[c_t(S)/c_0(S)]$ for the reaction of **7**–**9** with 9-Etgua as based on the ^1H NMR integral values of the δ-CH_3 protons. c_0(S) gives the initial concentration of the starting complexes **7**–**9**, c_t(S) their concentrations after *t* hours.

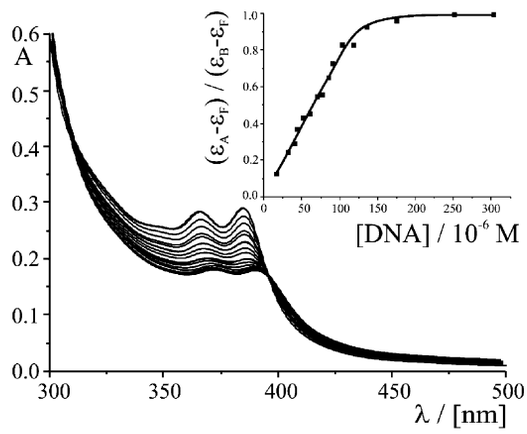

Fig. 5 UV-Vis spectra for the titration of $[(\eta^6\text{-}C_6Me_6)Ru(H_2metOMe)(dppz)](CF_3SO_3)_3$ **12** (20 μM) in a 10 mM phosphate buffer (pH 7.2) with CT DNA (0–300 μM (nucleotide)). The inset depicts the best least-squares fit to the model of Bard and Thorp[20,21] for this UV-vis titration.

the analogous Ir^{III} complex $[(\eta^5\text{-}C_5Me_5)Ir(AcmetOMe)(dppz)](CF_3SO_3)_2$ with its *k* value[7] of $1.64(11) \times 10^{-5}$ s^{-1}.

Fig. 5 depicts the UV-vis spectra recorded for a buffered 20 μM solution of $[(\eta^6\text{-}C_6Me_6)Ru(H_2metOMe)(dppz)]^{3+}$ (**12**) at pH 7.2 in the presence of increasing quantities of CT DNA. The observed average 39% decrease in absorbance (hypochromicity) at 366 and 385 nm and the bathochromic shifts (6 nm) of these absorption maxima are characteristic for strong intercalative DNA binding, as has been documented for other polypyridyl transition metal complexes.[19] An isosbestic point can be identified at 396 nm, in accordance with a simple equilibrium distribution between DNA-bound and free $(\eta^6\text{-}C_6Me_6)Ru^{II}$ complex **12**. UV absorption data recorded at 366 nm for the titration of **12** with CT DNA were fitted graphically using the model of Bard[20] and Thorp[21] to afford a least-squares estimate of $5.5(1) \times 10^6$ M^{-1} for the intrinsic binding constant K_b at an average binding site size *s* of 3.2 base pairs of DNA. This model assumes non-cooperative, non-specific binding with the existence of one type of discrete binding site, *i.e*. in this case an intercalation site. Calculations were performed for *s* values at 0.1 steps within the range $1 \leq s \leq 6$ with $s = 3.2$ providing the best least-squares fit to the experimental UV-vis titration data. Binding saturation is achieved at a [DNA]/[**12**] concentration ratio of 8 : 1 where [DNA] refers to M(nucleotide). Following the initial hypochromic shifts, on addition of a 15-fold excess of CT DNA to a 20 μM solution of **12** at pH 7.2 (see the final trace in Fig. 5), no change in the UV-vis spectrum of the final equilibrium mixture was observed over a period of 3 days. This was also the case at 15- to 25-fold CT DNA excess for the other complexes (**4**–**17**) studied in the course of this work. These observations indicate that the intercalative binding mode of

Table 1 Binding constants K_b, site sizes s and melting temperature shifts ΔT_m for the interaction of CT DNA with bioorganometallic complexes of the type $[(\eta^6\text{-arene})Ru(Aa)(dppz)]^{n+}$, n = 1–3. Buffer I (T_m = 70.1 °C) was employed for **7**–**12** and **15**–**17**, buffer II (T_m = 72.5 °C) for the remaining metal complexes. K_b values are for [DNA] concentrations in M(nucleotide) and are estimated to be accurate to within ±0.1 units for the given order of magnitude and binding site s. Experimental ΔT values are accurate to within ±1 °C

Complex	n	Arene	Aa	K_b/M^{-1}	s	ΔT_m/°C
4	1	C_6H_6	$AcH_{-1}cysOH$	5.3×10^4	1.6	7.2
5	1	$1,3,5\text{-}Me_3C_6H_3$	$AcH_{-1}cysOH$	1.2×10^5	1.7	11.3
6	1	C_6Me_6	$AcH_{-1}cysOH$	1.6×10^5	1.5	10.4
7	2	C_6H_6	AcmetOH	6.0×10^4	1.5	7.5
8	2	$1,3,5\text{-}Me_3C_6H_3$	AcmetOH	6.3×10^5	5.4	13.0
9	2	C_6Me_6	AcmetOH	7.3×10^5	5.1	18.4
10	3	C_6H_6	H_2metOMe	1.6×10^6	1.8	6.5
11	3	$1,3,5\text{-}Me_3C_6H_3$	H_2metOMe	1.7×10^6	2.8	11.5
12	3	C_6Me_6	H_2metOMe	5.5×10^6	3.2	18.2
13	1	C_6Me_6	$HglyglyH_{-1}cysOH$	1.5×10^5	4.6	9.4
14	2	C_6Me_6	HcysOMe	7.8×10^5	2.4	9.9
15	2	C_6Me_6	HglyglymetOH	9.9×10^5	2.3	18.5
16	3	*p*-cymene	H_2metOMe	1.4×10^5	2.5	5.7
17	3	$[9]aneS_3$	H_2metOMe	1.1×10^6	2.1	7.0

such $(\eta^6\text{-arene})Ru^{II}$ complexes is indeed strong enough to subdue any subsequent amino acid/peptide substitution caused by Ru–N covalent binding to DNA.

All the dppz complexes considered in this work exhibit well resolved absorption maxima in the range 350–400 nm (π–π* transitions), whose hypochromic shifts on titration with CT DNA can be analysed as for **12** by the model of Bard[20] and Thorp.[21] Binding constants K_b and corresponding site sizes s for the best least-squares fits to the UV-vis titration data of complexes **4**–**17** are listed in Table 1. The excellent agreement between experimental and calculated extinction values over the wide [DNA]/complex ranges depicted in Fig. 5 (**12**, 0–300 μM) and Fig. 6 (**7**–**9**, 0–450 μM) is typical for the UV-vis titrations

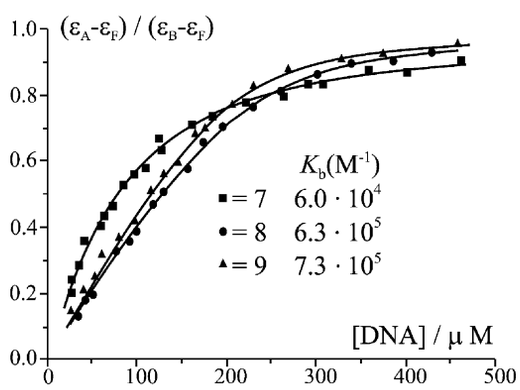

Fig. 6 Least-squares fits (Bard and Thorp)[20,21] to the UV-vis spectral data for the titrations of complexes $[(\eta^6\text{-arene})Ru(AcmetOH)(dppz)](CF_3SO_3)_2$ (arene = C_6H_6, $Me_3C_6H_3$, C_6Me_6, **7**–**9**) (20 μM) in a 10 mM phosphate buffer (pH 7.2) with CT DNA (0–450 μM(nucleotide)).

carried out during the course of this work. This finding and the fact that physically realistic binding site sizes in the range $1.5 \leq s \leq 5.4$ gave the best least-squares fits indicates that the Bard model provides an adequate description of the relatively strong to strong DNA binding observed for complexes **4**–**17**. K_b values can, of course, to some extent represent average values for different types of DNA interactions, particularly for lower binding constants ($< 2 \times 10^5$ M^{-1}). That this may well be the case for complexes **4**–**7** ($5.3 \times 10^4 \leq K_b \leq 1.6 \times 10^5$ M^{-1}) is indicated by the observation of rather low s values in the range 1.5 to 1.7. Binding site sizes less than unity are too small to account for the neighbour exclusion principle and have been interpreted as implying that intercalator ligands are stacking with one another on the DNA surface.[12,22]

The choice of complexes **4**–**17** allows a comparison of the influence of a) the net complex charge, b) the coligand, c) the number of amino acid residues, and d), by including our previous studies on $(\eta^5\text{-}C_5Me_5)M^{III}$, (M = Ir, Rh), compounds,[7] the nature of the half-sandwich fragment. The increase in K_b from 1.6×10^5 M^{-1} through 7.3×10^5 M^{-1} to 5.5×10^6 M^{-1} in the series of $(\eta^6\text{-}C_6Me_6)Ru^{II}$ complexes **6**, **9** and **12**, with their respective net charges of 1+, 2+ and 3+, clearly reflects a continuous strengthening of the electrostatic interaction with the negatively charged DNA phosphodiester backbone. Similar charge-dependent increases in K_b are observed for the analogous mesitylene (**5**, **8**, **11**) and benzene complexes (**4**, **7**, **10**). A comparable charge influence has recently been reported for a 3+ cobalt-sarcophagine cage complex[23] attached to an anthracene moiety, whose K_b value of 1.8×10^6 M^{-1} is some two orders of magnitude greater than that of the likewise intercalating (9-anthryl-methyl)ammonium (1+) cation.[24] On taking the additional $(\eta^6\text{-}C_6Me_6)Ru^{II}$ complexes **13**–**15** into account, it is apparent that the net cation charge is the major factor controlling the DNA binding constant in the bioorganometallic compounds considered in the present work. For instance, despite the possibility of additional hydrogen bonding introduced by the tripeptide ligand $HglyglyH_{-1}cysOH$ in the monocation of **13**, its observed K_b value of 1.5×10^5 M^{-1} is effectively identical to that of $[(\eta^6\text{-}C_6Me_6)Ru(AcH_{-1}cysOH)(dppz)]^+$ (**6**, $K_b = 1.6 \times 10^5$ M^{-1}). However, the 36% increase in K_b on going from $[(\eta^6\text{-}C_6Me_6)Ru(AcmetOH)(dppz)]^{2+}$ (**9**, $K_b = 7.3 \times 10^5$ M^{-1}) to $[(\eta^6\text{-}C_6Me_6)Ru(HglyglymetOH)(dppz)]^{2+}$ (**15**, $K_b = 9.9 \times 10^5$ M^{-1}) does, in contrast, suggest that N–H···X or O···H–X (X = N, O) peptide-to-duplex hydrogen bonds could in certain cases play a complementary role in stabilising the complex/DNA interaction. This finding is in accordance with our previous observation of a 66% increase in K_b for the analogous di-cationic $(\eta^5\text{-}C_5Me_5)Ir^{III}$ pair $[(\eta^5\text{-}C_5Me_5)Ir(AcmetOMe)(dppz)]^{2+}$/$[(\eta^5\text{-}C_5Me_5)Ir(HglyglymetOH)(dppz)]^{2+}$, for which similar DNA binding constants of 7.04×10^5 and 1.16×10^6 M^{-1} were determined.[7] It should also be noted that the binding site size s decreases from 5.1 to 2.3 on going from **9** to **15**, *i.e.* that more complex cations bind to DNA at saturation in the latter case.

With the exception of the dication $[(\eta^6\text{-}C_6H_6)Ru(AcmetOH)(dppz)]^{2+}$ (**7**), typical DNA binding constant ranges can be established for the $(\eta^6\text{-arene})Ru^{II}$ complexes **4**–**15**: 5.3×10^4–1.6×10^5 for monocations, 6.3×10^5–9.9×10^5 for dications and 1.6×10^6–5.5×10^6 for trications. The dominating role of the net cation charge is also reflected in the K_b value of 1.1×10^6 M^{-1} for $[([9]aneS_3\text{-}\kappa^3S)Ru(H_2metOMe)(dppz)]^{3+}$ (**17**), which lies just outside the above range for $(\eta^6\text{-arene})Ru^{II}$ half-sandwich complexes. Changing the transition metal fragment to $(\eta^5\text{-}C_5Me_5)Ir^{III}$ or $(\eta^5\text{-}C_5Me_5)Rh^{III}$ has effectively no influence on the efficacy of DNA binding,[7] a finding that is in striking contrast to the interaction behaviour of $[(\eta^6\text{-}p\text{-cymene})Ru(H_2metOMe)(dppz)]^{3+}$ (**16**). The remarkably low K_b value of

1.4×10^5 M^{-1} for this complex must be ascribed to the bulkiness of the arene *iso*-propyl substituent, which appears to hinder effective electrostatic interactions and/or intercalation.

A significant trend to higher DNA binding constants is clearly apparent from Table 1 for the coligand series benzene < mesitylene < hexamethylbenzene. For instance, K_b for the trication of **12** is some 3.2 times higher than that for the analogous mesitylene complex **11**. A possible explanation is that the increase in electron density within the dppz dipyridine system along the (η^6-arene)Ru^{II} series **4**–**6**, **7**–**9** and **10**–**12** could lead to improved electron correlation between DNA nucleobases and the intercalating ligand. However, as previously discussed for the *p*-cymene complex **16**, the DNA binding behaviour of such bioorganometallic half-sandwich compounds can also be influenced by the steric requirements of their arene substituents. Fig. 6 depicts the least-squares fits to UV-vis spectral data for the titration of the dicationic AcmetOH complexes **7**–**9** with CT DNA. Due to the reduced bulkiness of its η^6-benzene ligand, DNA binding of complex **7** is clearly more efficient than that of **8** or **9** at CT DNA/complex ratios below *ca.* 9 : 1. In contrast, at CT DNA concentrations above *ca.* 200 μM, the improved electron correlation between the dppz ligand and DNA nucleobases leads to the observed higher K_b values for the mesitylene and hexamethylbenzene complexes. The significant increase in the binding site size *s* from 1.5 in **7** to respectively 5.4 and 5.1 in **8** and **9** is also in accordance not only with the bulkier nature of the η^6-arene ligand in the latter two complexes but also with improved DNA intercalation. This parameter *s* can be regarded as giving an estimate of the average number of nucleobase pairs between neighbouring intercalating dppz ligands.

Although a consistent trend to higher K_b values is apparent on going from mesitylene to hexamethylbenzene half-sandwich complexes, the relative increase in K_b is modest in all cases in comparison to that observed for the benzene/mesitylene pairs **4/5** (AcH_{-1}cysOH) and **7/8** (AcmetOH). Possible explanations for this state of affairs are that the intercalation binding energy for the dppz ligand might be similar in both η^6-$Me_3C_6H_3$ and η^6-C_6Me_6 complexes or that an optimal DNA interaction with improved electron correlation in the latter compounds is hampered by the increased steric requirements of hexamethylbenzene. Thermal denaturation studies for CT DNA should provide a means of gauging the efficacy of dppz intercalation, provided that electrostatic and hydrogen bonding interactions can be regarded as remaining effectively unaffected by any coligand variation. Fig. 7 depicts the UV-vis spectra for a CT DNA/complex **15** mixture (10 : 1 molar ratio) taken at increasing temperatures and Fig. 8 the thermal denaturation curves of A_{260} for similar CT DNA/complex mixtures containing the tricationic complexes [(η^6-arene)Ru(H_2metOMe)(dppz)]-(CF_3SO_3)$_3$ **10**–**12**. The dramatic and systematic increase in the

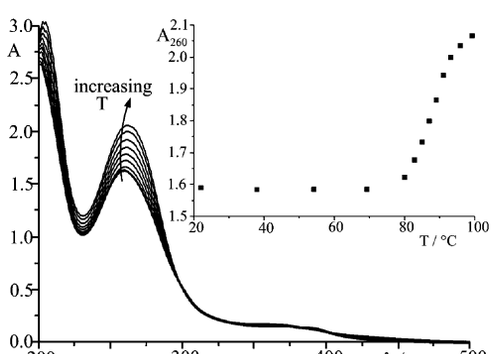

Fig. 7 UV-Vis spectra for the thermal denaturation of a 10 : 1 molar ratio of CT DNA/[(η^6-C_6Me_6)Ru(HglyglymetOH)(dppz)](CF_3SO_3)$_2$ mixture in a 10 mM phosphate/20 mM NaCl buffer at pH 7.2. The inset depicts the thermal denaturation curve for the UV absorbance A_{260} at 260 nm.

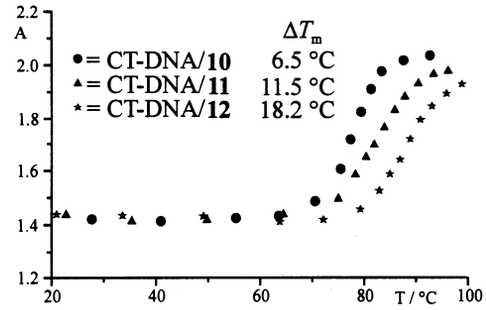

Fig. 8 Comparison of the thermal denaturation curves for (A_{260} *vs.* temperature) for CT DNA/complex mixtures (10 : 1 molar ratio with [DNA] in M(nucleotide)) of compounds [(η^6-arene)Ru(H_2metOMe)-(dppz)](CF_3SO_3)$_3$ (arene = C_6H_6, $Me_3C_6H_3$, C_6Me_6, **10**–**12**) in buffer I. T_m for CT-DNA in buffer I is 70.1 °C.

DNA melting temperature within this series (ΔT_m = 6.5 (**10**), 11.5 (**11**), 18.2 °C (**12**)) is in accordance with a steady increase in the intercalative binding energy, *i.e.* with improved π-stacking for dppz ligands and neighbouring DNA nucleobases within the duplex. A similar trend (ΔT_m = 7.5, 13.0, 18.4 °C) is observed for the dicationic AcmetOH series **7**–**9**, thereby clearly indicating that electrostatic interactions can only play a lesser role in causing the very high ΔT_m values recorded for the η^6-C_6Me_6 complexes **9** and **12**. This interpretation is also supported by the remarkable increase of 18.5 °C in the denaturation temperature of CT DNA in the presence of the dicationic complex [(η^6-C_6Me_6)Ru(HglyglymetOH)(dppz)](CF_3SO_3)$_2$ (**15**) (see Fig. 7). As listed in Table 1, the lower ΔT_m values for the tricationic *p*-cymene and [9]aneS_3 complexes **16** and **17** (5.7, 7.0 °C) are closely similar to those of the η^6-C_6H_6 complexes **7** and **10** (7.5, 6.5 °C).

The ΔT_m values for the η^6-C_6Me_6 complexes **9**, **12** and **15** are significantly higher than that of 9.1 °C[12] for [Ru(phen)$_2$-(dppz)]$^{2+}$ or those of 10–14 °C reported for other metallointercalators.[25,26] This suggests that electron correlation between the dipyridyl part of dppz and polar regions of the duplex nucleobases may be particularly effective for η^6-C_6Me_6 half-sandwich complexes. The possible mode of DNA interaction was studied by two-dimensional NOESY for [(η^6-C_6-Me_6)Ru(AcmetOH)(dppz)]$^{2+}$ (**9**) with the self-complementary oligonucleotide d(GTCGAC)$_2$. This investigation also enables a comparison with Δ-[Ru(phen)$_2$(dppz)]$^{2+}$, Δ-[Ru(phen)$_2$(dpq)]$^{2+}$ (dpq = dipyrido[3,2-*d*:2′,3′-*f*]quinoxaline) and [(η^5-C_5Me_5)-Ir(H_2metOMe)(dppz)]$^{3+}$, whose intercalative binding to d(GTCGAC)$_2$ has previously been studied by NMR techniques.[4,7,27–29] In accordance with these reports, the fact that the NOE cross peak from each purine/pyrimidine H8/H6 to its own sugar H2′ proton is significantly larger than that to the adjacent H2′ proton (Fig. 9) confirms the adoption of a B-type duplex conformation by d(GTCGAC)$_2$.

Addition of **9** to the hexanucleotide at a 0.8 : 1 molar ratio at 283 K induces marked upfield shifts and broadening of the dppz proton resonances (Fig. 10), both of which phenomena are clearly indicative of intercalative binding by the polypyridyl ligand. The larger ^{1}H NMR shifts of −0.35 and −0.28 ppm for the respective atom pairs H4/H7 and H11/H14 suggest that these protons must penetrate to a greater extent into the base stack, than their H3/H8 (−0.16 ppm), H12/H13 (−0.15 ppm) and H2/H9 (−0.06 ppm) counterparts. In the 300 ms NOESY spectrum depicted in Fig. 10, new NOE cross peaks appear for the dppz H2/H9 and H3/H8 proton pairs with respectively CH_3-T_2 and H_2′-G_1. A further dppz-nucleobase NOE cross peak is observed at 9.28/8.01 ppm for the H2/H9 pair and a guanine H8. The presence of these NOEs is consistent with a sequence-selective intercalation at G_1T_2/C_6A_5 in the major groove, as also previously reported[7] for [(η^5-C_5Me_5)Ir(H_2-metOMe)(dppz)]$^{3+}$. Of particular interest in this respect are two additional, presumably H6-T_2 NOEs, at 7.53/1.75 and 7.53/1.95

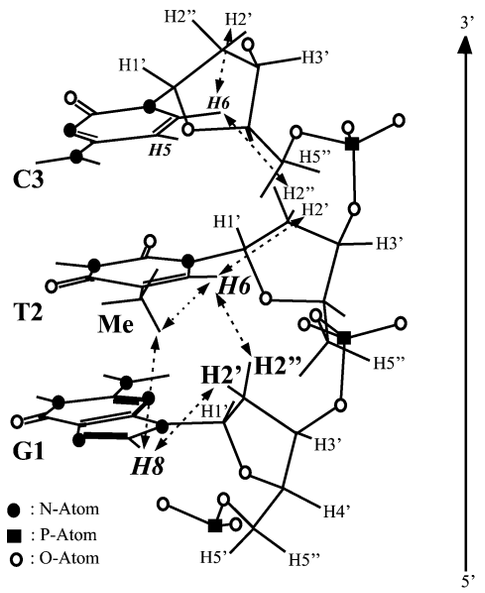

Fig. 9 5′-GTC-3′ segment of the d(GTCGAC)$_2$ hexamer.

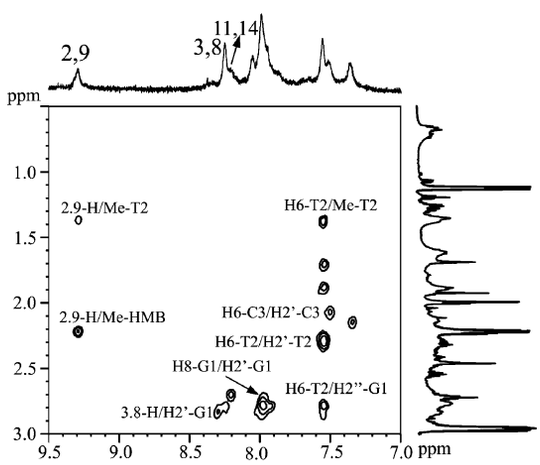

Fig. 10 Section of the 300 ms 2D NOESY spectrum of the [(η^6-C_6Me_6)Ru(AcmetOH)(dppz)](CF_3SO_3)$_2$–d(GTCGAC)$_2$ reaction mixture (molar ratio 0.8 : 1) in a 10 mM phosphate buffer [pH 7.2] at 283 K.

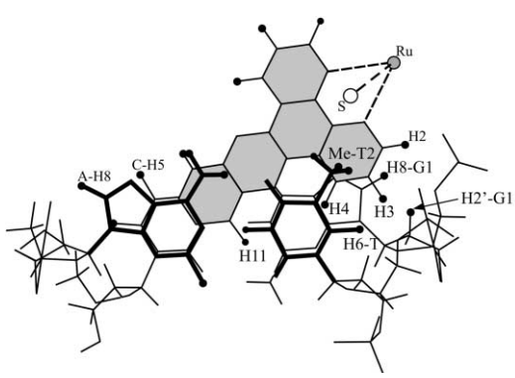

Fig. 11 Schematic depiction of a possible side-on intercalation of [(η^6-C_6Me_6)Ru(AcmetOH)(dppz)](CF_3SO_3)$_2$ (**9**) into the G_1T_2/C_6A_5 sequence of the hexanucleotide d(GTCGAC)$_2$.

ppm, that may be due to the proximity of the AcmetOH β-CH_2 protons. Taken as a whole, the observed chemical shifts and NOEs are in accordance with the site-specific intercalation mode for complex **9** proposed in Fig. 11. Such a side-on[30] intercalation would enable short 2,9-H/Me-T_2, 2,9-H/H8-G_1 and 3,8-H/H2′-G_1 dppz/oligonucleotide contacts. Furthermore, it is just the charge distribution at the 2,9 and 3,8 carbon atoms of the dppz dipyridyl units that is most directly affected by coligand variation in the (η^6-arene)Ru^{II} half-sandwich complexes.

It is interesting to compare our present findings with those of other NMR studies on the intercalation of Ru^{II} complexes into d(GTCGAC)$_2$. Major groove binding was also proposed by Dupureur and Barton[4] for the complex Δ-[Ru(phen)$_2$(dppz)]$^{2+}$ on the basis of an NOE from dppz 4,7-H to H8-A_5 of the hexanucleotide. In contrast, the pattern of intermolecular NOEs recorded by Collins *et al.*[31] in their recent binding study for Δ-[Ru(Me_2phen)$_2$(dppz)]$^{2+}$ clearly indicates that the analogous 2,9-dimethyl-1,10-phenathroline complex intercalates from the minor groove, in accordance with an original proposal for Δ-[Ru(phen)$_2$(dppz)]$^{2+}$ from Lincoln *et al.*[32] NOE cross peaks were observed from the Me_2phen methyl protons to the hexanucleotide minor groove sugar H1′ and H4′/H5′/H5″ protons and from dppz H11/H14 and H12/H13 to the major groove H2′-G_4, H2′/2″-G_1 and Me-T_2 protons. This suggests that the methyl protons must be located in the minor groove and that the intercalating dppz ligand projects out into the opposite major groove. The front-on deep dppz penetration is also indicated by the magnitude of the upfield ^{1}H NMR shifts of respectively −0.51 and −0.67 ppm for H3/H8 and H4/H7 at the middle of the base stack in comparison to H11/H14 (−0.42) and H12/H13 (−0.35) on the major groove side. This NOE pattern is clearly in striking contrast to that of [(η^6-C_6H_6)-Ru(AcmetOH)(dppz)]$^{2+}$ (**9**) whose 2,9-H/Me-T_2, 2,9-H/H8-G_1 and 3,8-H/H2′-G_1 intermolecular NOEs and modest dppz H3/H8 and H4/H7 upfield shifts of respectively −0.35 and −0.16 ppm can only be accounted for by the proposed major groove side-on intercalation mode. Although our NMR results are only consistent with a sequence-selective interaction at G_1T_2/C_6A_5, the fact that the H4/H7 and H11/H14 protons shift as pairs suggests that the metal complex must exchange relatively rapidly between various binding modes, *i.e.* that the observed NOEs themselves only provide a time-averaged representation of the binding of **9** to the hexanucleotide.

Our findings for (η^5-C_5Me_5)Ir^{III} and (η^6-arene)Ru^{II} complexes indicate that the preferred groove for DNA binding by metallointercalators will most likely be influenced not only by the shape of the intercalating ligand but also by the steric bulk of the other participating ligands in the metal coordination sphere. The presence of relatively bulky η^5- or η^6-coordinated arenes instead of phen derivatives appears to disfavour front-on intercalation and deeper dppz penetration. However, as indicated by the remarkably high ΔT_m values of 18.4 °C for CT DNA in the presence of complex **9**, specific dipolar major groove intercalative interactions between the dipyridyl moiety of dppz and the DNA nucleobases can apparently promote duplex stabilisation in a highly efficient manner despite a lack of deep dppz penetration.

Experimental

Materials

Amino acids (AccysOH, AcmetOH, HmetOMe; HcysOH = cysteine, HmetOH = methionine), and peptides (HglyglycysOH; HglyOH = glycine) were purchased from Bachem (Heidelberg) and used as received, as were calf thymus DNA (CT DNA) from Sigma and the hexanucleotide d(GTCGAC)$_2$ from Life Technologies. $RuCl_3 \cdot xH_2O$ was obtained from Chempur, hexamethylbenzene, mesitylene (Mes), α-phellandrene, 1,3-cyclohexadiene and 1,10-phenanthroline from Merck. The starting compounds [{(η^6-arene)RuCl(μ-Cl)}$_2$] (arene = C_6H_6, $Me_3C_6H_3$ (Mes), C_6Me_6, *p*-cymene (Cy)) and [([9]aneS_3)-RuCl(dppz)]Cl were prepared in accordance with literature procedures.[33–35] Dipyrido[3,2-*a*:2′,3′-*c*]phenazine (dppz) was synthesised from 1,10-phenanthroline by the method of ref. 36. All solvents were analytical reagents grade (J.T. Baker) and were dried and distilled before use.

Spectroscopic measurements

FAB mass spectra were recorded on a Fisons VG Autospec employing 3-nitrobenzyl alcohol as the matrix, UV-vis spectra on a Perkin-Elmer Lambda 15 spectrometer, IR spectra as KBr discs on a Perkin-Elmer 1760. Microanalyses (C, H, N and S) were performed using a Vario EL elemental analyser (Elementar Analysensysteme). ^{1}H NMR spectra were recorded on Bruker DRX 400 and DRX 600 spectrometers using 5 mm tubes, ^{13}C NMR on the DRX 400. Chemical shifts are reported as δ values relative to the signal of the deuterated solvent. 2D-NOESY spectra were acquired on the DRX 600 at 283 K with a mixing time of 300 ms using 2.5 mm tubes and referenced to sodium 3-(trimethylsilyl)tetradeuteriopropionate (TSP).

DNA binding studies

The thermal denaturation temperature of complex/DNA mixtures (1 : 10) was determined either in buffer I (10 mM phosphate buffer, pH 7.2) for the methionine derivatives **7**–**12** or in buffer II (10 mM phosphate buffer, 20 mM NaCl, pH 7.2) for the cysteine derivatives **4**–**6** and **14**. Melting curves were recorded at 260 nm on a Lambda 15 Perkin-Elmer spectrophotometer connected with a temperature controller (HAAKE FS thermostat). A ramp rate of 0.25 °C min^{-1} was used over the range 25–96 °C. The melting temperatures of the native and modified DNA were calculated by determining the midpoints of the melting curves from the first-order derivatives. Experimental ΔT_m values are estimated to be accurate within ±1 °C. The NaCl free buffer I was used for met derivatives to prevent possible substitution of the amino acid or peptide by chloride ions. The concentrations of the nucleic acids d(GTCGAC)$_2$ and CT DNA were determined spectrophotometrically by using the molar extinction coefficient[37] $\varepsilon_{260\ nm}$ = 6600 M^{-1} cm^{-1}. All absorption titrations were carried out at room temperature. After sonication, the solutions of CT DNA in the appropriate buffer gave a ratio of UV absorbance at A_{260}/A_{280} of *ca*. 1.90, indicating that DNA was sufficiently free of protein.[38] Fixed amounts of metal complexes were titrated with DNA over a range of DNA concentrations from 0 to 300–450 μM (nucleotide) with the higher value being employed for titrations in which binding saturation was not fully achieved. All UV spectra were measured after equilibration (no further change in the monitoring absorbance). Titration curves were constructed from the fractional change in the absorption intensity as a function of DNA concentration according to the model of Bard[20] and Thorp[21] for non-cooperative non-specific binding for one type of discrete DNA binding site. Eqn. (1) was used to fit the absorption data by least-squares refinement of binding constants (K_b) and site sizes (s):

$$(\varepsilon_a - \varepsilon_f)/(\varepsilon_b - \varepsilon_f) = (b - \{b^2 - 2K_b^2C_t[\mathrm{DNA}]/s\}^{1/2})/2K_bC_t \quad (1)$$

$$b = 1 + K_bC_t + K_b[\mathrm{DNA}]/2s$$

where ε_a is the extinction coefficient observed at a given DNA concentration, ε_f the extinction coefficient of the complex in the absence of DNA, ε_b the extinction coefficient of the complex when fully bound to DNA (no absorption change on further addition of DNA), K_b the equilibrium binding constant in M^{-1}, C_t the total metal complex concentration, [DNA] the DNA concentration in M (nucleotide), and s the binding site size. Values of ε_b were obtained by extrapolation from the y intercept of plots of $\varepsilon_a/\varepsilon_f$ versus 1/[DNA]. Fits of experimental absorption titrations were performed by use of the program ORIGIN 6.0 for s values varied at 0.1 steps in the range $1 \leq s \leq 6$. The K_b and s values of Table 1 provided the best least-squares fits to individual experimental UV-vis titration curves. Standard deviations in the range 0.03–0.07 units for the given order of magnitude were obtained for the binding constants K_b.

Kinetic measurements

^{1}H NMR kinetic measurements were used to obtain the rate constant of the intermolecular substitution of AcmetOH in the thioether metal complexes [(η^6-C$_6$H$_6$)Ru(AcmetOH)(dppz)]$^{2+}$ **7**, [(η^6-Mes)Ru(AcmetOH)(dppz)]$^{2+}$ **8** and [(η^6-C$_6$Me$_6$)Ru(AcmetOH)(dppz)]$^{2+}$ **9** by N7 of the nucleobase 9-ethylguanine. The reactions were carried out in phosphate buffer (10 mM, pH 7.2) using D$_2$O as a solvent. ^{1}H NMR spectra were recorded at 298 K over a peroid of 200 h.

Syntheses

All reactions were carried out under argon using standard Schlenk techniques. The starting compounds [(η^6-C$_6$H$_6$)Ru(acetone)(dppz)](CF$_3$SO$_3$)$_2$ **1a**, [(η^6-Mes)Ru(acetone)(dppz)](CF$_3$SO$_3$)$_2$ **2a** and [(η^6-C$_6$Me$_6$)Ru(acetone)(dppz)](CF$_3$SO$_3$)$_2$ **3a** were prepared from respectively [(η^6-C$_6$H$_6$)RuCl(dppz)]Cl **1**, [(η^6-Mes)RuCl(dppz)]Cl **2** and [(η^6-C$_6$Me$_6$)RuCl(dppz)]Cl **3** by stirring these with an equivalent quantity of Ag(CF$_3$SO$_3$) in acetone and subsequently filtering of the precipitated AgCl. Complexes **4**–**17** were then prepared by one of the three following general methods:

Method A

0.1 mmol of the starting compound (**1a**, **2a** or **3a**) and an equivalent quantity of amino acid (AccysOH, AcmetOH) were mixed in 10 ml CH$_3$OH–CH$_2$Cl$_2$ (1 : 10) (AccysOH) or 10 ml acetone (AcmetOH). The solution reaction was stirred for the designated time and temperature. After reduction of the solvent volume to *ca*. 4 ml, addition of diethyl ether led to precipitation of the desired product, which was washed three times with diethyl ether and dried at 50 °C *in vacuo*.

Method B

A solution of HcysOMe·HCl or HmetOMe·HCl (0.1 mmol) in 5 ml methanol (HcysOMe·HCl) or acetone (HmetOMe·HCl) was stirred with 0.1 mmol Ag(CF$_3$SO$_3$) for 30 min and the precipitated AgCl removed by centrifugation at 5 °C. The preparation of the complexes was then performed in a manner similar to Method A.

Method C

0.1 mmol of the starting material **3a** were dissolved in 10 ml water. Addition of 0.1 mmol peptide (HglyglymetOH or HglyglycysOH) provided a suspension which was stirred for the designated time and temperature. The solvent was removed and the remaining solid dissolved in 3 ml methanol. After addition of diethyl ether the resulting precipitate was washed three times with Et$_2$O and dried for several hours at 50 °C *in vacuo*.

[(η^6-C$_6$H$_6$)RuCl(dppz)]Cl 1. After stirring of an ethanol solution of 500 mg [{(η^6-C$_6$H$_6$)RuCl(μ-Cl)}$_2$] (1 mol) and 305.6 mg dppz (1.05 mol) for 1 h at 60 °C, the resulting off-yellow precipitate of **1** was filtered off and dried *in vacuo*. Yield 1.02 g, 94% (Found: C, 53.9; H, 3.3; N, 10.2. Calc. for C$_{24}$H$_{16}$Cl$_2$N$_4$Ru: C, 54.1; H, 3.0; N, 10.5%). FAB mass spectrum: *m*/*z* 418.8 (20%, [M − C$_6$H$_6$ − Cl]$^+$) and 496.9 (100, [M − Cl]$^+$). ^{1}H NMR (CD$_3$OD): δ 6.34 (s, 6H, C$_6$H$_6$), 8.15 (dd, 2H), 8.28 (dd, 2H), 8.50 (dd, 2H), 9.89 (dd, 2H), 10.02 (dd, 2H, dppz). ^{13}C NMR (CD$_3$OD): δ 88.7 (C$_6$H$_6$), 128.9, 131.1, 132.0, 133.9, 137.4, 140.6, 144.4, 158.6 (dppz).

[(η^6-Mes)RuCl(dppz)]Cl 2. Preparation as for **1** with [{η^6-Mes)RuCl(μ-Cl)}$_2$] and dppz. Yield 975.8 mg, 85% (Found: C, 56.3; H, 4.3; N, 10.2. Calc. for C$_{27}$H$_{22}$Cl$_2$N$_4$Ru: C, 56.5; H, 3.9; N, 9.8%). FAB mass spectrum: *m*/*z* 418.9 (25%, [M − Mes − Cl]$^+$) and 539.0 (100, [M − Cl]$^+$). ^{1}H NMR (CD$_3$OD): δ 2.36 (s, 9H, Mes), 5.7 (s, 3H, Mes), 8.13 (dd, 2H), 8.29 (dd, 2H), 8.47

(dd, 2H), 9.83 (mm, 4H, dppz). ^{13}C NMR (CD_3OD): δ 19.2 (Mes), 81.2 (Mes), 108.9 (Mes), 129.0, 131.1, 131.5, 133.8, 137.2, 140.8, 144.4, 157.7 (dppz).

[(η^6-C_6Me_6)RuCl(dppz)]Cl 3. Preparation as for **1** with [{η^6-C_6Me_6)RuCl(μ-Cl)}$_2$] and dppz. Yield 1.11 g, 90% (Found: C, 57.9; H, 4.9; N, 8.9. Calc. for $C_{30}H_{28}Cl_2N_4Ru$: C, 58.4; H, 4.6; N, 9.1%). FAB mass spectrum: *m*/*z* 581.1 (100, $[M - Cl]^+$). ^{1}H NMR (CD_3OD): δ 2.27 (s, 18H, C_6Me_6), 8.05 (dd, 2H), 8.31 (mm, 4H), 9.46 (dd, 2H), 9.68 (dd, 2H, dppz). ^{13}C NMR (CD_3OD): δ 16.2 (C_6Me_6), 97.8 (C_6Me_6), 129.1, 131.0, 131.5, 133.8, 137.0, 140.8, 144.2, 156.5 (dppz). Crystals of [(η^6-C_6Me_6)-RuCl(dppz)](CF_3SO_3) **3b** were prepared by gas diffusion (diethyl ether–methanol) following addition of an equiv. of Ag(CF_3SO_3) and AgCl removal.

[(η^6-C_6H_6)Ru(AcH$_{-1}$cysOH)(dppz)](CF_3SO_3) 4. Method A, 18 h, 45 °C. Yield 40.95 mg, 53% (Found: C, 46.1; H, 3.4; N, 9.1; S, 8.6. Calc. for $C_{30}H_{24}F_3N_5O_6RuS_2$: C, 46.6; H, 3.1; N, 9.1; S, 8.3%). FAB mass spectrum: *m*/*z* 461.9 (100, [(η^6-C_6H_6)-Ru(dppz)]$^+$), 610.8 (20, $[M - AcH_{-1}cysOH]^+$) and 625.0 (8%, $[M - CF_3SO_3]^+$). ^{1}H NMR (CD_3OD): δ 1.90 (s, 3H, CH_3 Ac), 2.65 (mm, 2H, β-CH_2), 3.02 (br, 1H, α-CH), 6.32 (s, 6H, C_6H_6), 8.1 (mm, 4H), 8.35 (m, 2H), 9.7 (mm, 4H, dppz). ^{13}C NMR (CD_3OD): δ 22.4 (CH_3 Ac), 36.4 (β-CH_2), 56.8 (α-CH), 90.8 (C_6H_6), 128.9, 131.0, 132.1, 133.9, 137.2, 140.4, 144.1, 149.8, 158.7 (dppz), 171.7, 172.9 (CO). $\tilde{\nu}_{max}$/cm^{-1} 1734, 1653 (νCO), 1540 (δNH).

[(η^6-Mes)Ru(AcH$_{-1}$cysOH)(dppz)](CF_3SO_3) 5. Method A, 18 h, 45 °C. Yield 41.55 mg, 51% (Found: C, 48.2; H, 3.8; N, 8.3; S, 7.8. Calc. for $C_{33}H_{30}F_3N_5O_6RuS_2$: C, 48.6; H, 3.7; N, 8.6; S, 7.9%). FAB mass spectrum: *m*/*z* 504.0 (100, [(η^6-Mes)-Ru(dppz)]$^+$) and 666.0 (30%, $[M - CF_3SO_3]^+$). ^{1}H NMR (CD_3OD): δ 1.5 (br, 3H, CH_3 Ac), 1.8 (br, 1H, β-CH_2), 2.1 (br, 1H, β-CH_2), 2.26 (s, 9H, Mes), 3.03 (br, 1H, α-CH), 5.69 (s, 3H, Mes), 8.2 (mm, 4H), 8.5 (m, 2H), 9.41 (m, 2H), 9.85 (m, 2H, dppz). ^{13}C NMR (CD_3OD): δ 19.0 (Mes), 22.3 (CH_3 Ac), 35.5 (β-CH_2), 56.9 (α-CH), 83.8 (Mes), 112.1 (Mes), 129.2, 129.8, 131.2, 132.5, 134.0, 137.4, 141.0, 144.5, 150.5, 157.5, 158.1 (dppz), 171.8, 172.8 (CO). $\tilde{\nu}_{max}$/cm^{-1} 1734, 1653 (νCO), 1541 (δNH).

[(η^6-C_6Me_6)Ru(AcH$_{-1}$cysOH)(dppz)](CF_3SO_3) 6. Method A, 18 h, 45 °C. Yield 45.63 mg, 56% (Found: C, 50.4; H, 3.9; N, 7.8; S, 8.0. Calc. for $C_{36}H_{36}F_3N_5O_6RuS_2$: C, 50.5; H, 4.2; N, 8.2; S, 7.5%). FAB mass spectrum: *m*/*z* 546.0 (100, [(η^6-C_6Me_6)-Ru(dppz)]$^+$) and 708.3 (60%, $[M - CF_3SO_3]^+$). ^{1}H NMR (CD_3OD): δ 1.3 (br, 2H, β-CH_2), 1.78 (br, 3H, CH_3 Ac), 2.19 (s, 18H, C_6Me_6), 3.0 (br, 1H, α-CH), 8.15 (m, 2H), 8.25 (m, 2H), 8.51 (m, 2H), 9.25 (m, 2H), 9.84 (m, 2H, dppz). ^{13}C NMR (CD_3OD): δ 15.7 (C_6Me_6), 22.3 (CH_3 Ac), 27.8 (β-CH_2), 56.7 (α-CH), 98.9 (C_6Me_6), 128.9, 130.0, 131.2, 133.9, 134.1, 136.5, 141.4, 144.6, 149.9, 156.8, 157.0 (dppz), 171.8, 172.8 (CO). $\tilde{\nu}_{max}$/cm^{-1} 1742, 1652 (νCO), 1539 (δNH).

[(η^6-C_6H_6)Ru(AcmetOH)(dppz)](CF_3SO_3)$_2$ 7. Method A, 18 h, 60 °C. Yield 49.4 mg, 52% (Found: C, 41.4; H, 3.4; N, 6.9; S, 10.0. Calc. for $C_{33}H_{29}F_6N_5O_9RuS_3$: C, 41.7; H, 3.1; N, 7.4; S, 10.1%). FAB mass spectrum: *m*/*z* 462.0 (20, [(η^6-C_6H_6)-Ru(dppz)]$^+$), 610.9 (100, [(η^6-C_6H_6)Ru(dppz) + $CF_3SO_3]^+$), 652.0 (20, $[M - 2CF_3SO_3]^+$) and 802.0 (15%, $[M - CF_3SO_3]^+$). ^{1}H NMR (CD_3OD): δ 1.83 (m, 1H, β-CH_2), 1.88 (s, 3H, CH_3 Ac), 2.07 (m, 1H, β-CH_2), 2.12 (s, 3H, δ-CH_3), 2.4 (mm, 2H, γ-CH_2), 4.27 (dd, 1H, α-CH), 6.63 (s, 6H, C_6H_6), 8.18 (dd, 2H), 8.37 (m, 2H), 8.55 (dd, 2H), 9.89 (m, 2H), 10.03 (m, 2H, dppz). ^{13}C NMR (CD_3OD): δ 20.5 (δ-CH_3), 22.8 (CH_3 Ac), 30.8 (β-CH_2), 37.4 (γ-CH_2), 51.7 (α-CH), 92.5 (C_6H_6), 129.8, 131.2, 133.3, 134.2, 138.8, 140.8, 144.7, 150.8, 159.7 (dppz), 173.4, 173.8 (CO). $\tilde{\nu}_{max}$/cm^{-1} 1734, 1662 (νCO), 1548 (δNH).

[(η^6-Mes)Ru(AcmetOH)(dppz)](CF_3SO_3)$_2$ 8. Method A, 18 h, 60 °C. Yield 62.6 mg, 63% (Found: C, 43.1; H, 3.7; N, 6.5; S, 8.9. Calc. for $C_{36}H_{35}F_6N_5O_9RuS_3$: C, 43.1; H, 3.7; N, 6.5; S, 8.9%). FAB mass spectrum: *m*/*z* 504.0 (100, [(η^6-Mes)Ru(dppz)]$^+$), 652.9 (30, [(η^6-Mes)Ru(dppz) + $CF_3SO_3]^+$) and 843.9 (5%, $[M - CF_3SO_3]^+$). ^{1}H NMR (CD_3OD): δ 1.78 (s, 3H, δ-CH_3), 1.8 (mm, 3H, β-CH_2 and γ-CH_2), 1.89 (s, 3H, CH_3 Ac), 2.0 (mm, 1H, β-CH_2), 2.35 (s, 9H, Mes), 4.29 (br, 1H, α-CH), 6.01 (s, 3H, Mes), 8.19 (dd, 2H), 8.40 (m, 2H), 8.56 (dd, 2H), 9.70 (m, 2H), 10.04 (m, 2H, dppz). ^{13}C NMR (CD_3OD): δ 18.6 (δ-CH_3), 18.9 (Mes), 22.8 (CH_3 Ac), 30.5 (β-CH_2), 34.5 (γ-CH_2), 52.0 (α-CH), 84.3 (Mes), 115.4 (Mes), 129.8, 131.2, 133.0, 134.1, 138.7, 141.0, 144.6, 151.1, 158.4 (dppz), 173.5, 173.8 (CO). $\tilde{\nu}_{max}$/cm^{-1} 1734, 1663 (νCO), 1540 (δNH).

[(η^6-C_6Me_6)Ru(AcmetOH)(dppz)](CF_3SO_3)$_2$ 9. Method A, 18 h, 60 °C. Yield 72.5 mg, 70% (Found: C, 45.1; H, 3.8; N, 6.6; S, 8.9. Calc. for $C_{39}H_{41}F_6N_5O_9RuS_3$: C, 45.3; H, 4.0; N, 6.8; S, 9.3%). FAB mass spectrum: *m*/*z* 546.1 (100, [(η^6-C_6Me_6)-Ru(dppz)]$^+$), 695.1 (45, [(η^6-C_6Me_6)Ru(dppz) + $CF_3SO_3]^+$), 736.1 (30, $[M - 2CF_3SO_3]^+$ and 886.1 (10%, $[M - CF_3SO_3]^+$). ^{1}H NMR (CD_3OD): δ 1.65 (s, 3H, δ-CH_3), 1.8 (mm, 3H, β- and γ-CH_2), 1.93 (s, 3H, CH_3 Ac), 2.0 (m, 1H, β-CH_2), 2.3 (s, 18H, C_6Me_6), 4.38 (br, 1H, α-CH), 8.20 (m, 2H), 8.43 (m, 2H), 8.57 (m, 2H), 9.42 (m, 2H), 10.05 (m, 2H, dppz). ^{13}C NMR (CD_3OD): δ 16.0 (C_6Me_6), 16.7 (δ-CH_3), 22.8 (CH_3 Ac), 30.6 (β-CH_2), 33.9 (γ-CH_2), 51.9 (α-CH), 103.2 (C_6Me_6), 129.9, 131.2, 133.3, 134.2, 138.6, 141.1, 144.7, 150.7, 157.3 (dppz), 173.6, 173.8 (CO). $\tilde{\nu}_{max}$/cm^{-1} 1749, 1636 (νCO), 1541 (δNH).

[(η^6-C_6H_6)Ru(H$_2$metOMe)(dppz)](CF_3SO_3)$_3$ 10. Method B, 18 h, 60 °C. Yield 70.8 mg, 66% (Found: C, 36.5; H, 2.9; N, 6.2; S, 11.8. Calc. for $C_{33}H_{30}F_9N_5O_{11}RuS_4$: C, 36.9; H, 2.8; N, 6.5; S, 12.0%). FAB mass spectrum: *m*/*z* 461.9 (100, [(η^6-C_6H_6)Ru(dppz)]$^+$), 610.8 (65, [(η^6-C_6H_6)Ru(dppz) + $CF_3SO_3]^+$), 695.8 (15, $[M - C_6H_6 - 2CF_3SO_3]^+$), 773.8 (4, $[M - 2CF_3SO_3]^+$) and 923.8 (8%, $[M - CF_3SO_3]^+$). ^{1}H NMR (CD_3OD): δ 2.06 (s, 3H, δ-CH_3), 2.1 (mm, 2H, β-CH_2), 2.7 (mm, 2H, γ-CH_2), 3.77 (s, 3H, CH_3 OMe), 3.99 (dd, 1H, α-CH), 6.65 (s, 6H, C_6H_6), 8.19 (dd, 2H), 8.38 (dd, 2H), 8.55 (dd, 2H), 9.93 (m, 2H), 10.04 (m, 2H, dppz). ^{13}C NMR (CD_3OD): δ 19.9 (δ-CH_3), 29.2 (β-CH_2), 36.5 (γ-CH_2), 52.3 (α-CH), 54.4 (CH_3 OMe), 92.6 (C_6H_6), 129.8, 131.2, 133.3, 134.1, 138.8, 139.0, 140.8, 144.7, 150.9, 159.8 (dppz), 169.6 (COO). $\tilde{\nu}_{max}$/cm^{-1} 1749 (νCO), 1636, 1539 (δNH).

[(η^6-Mes)Ru(H$_2$metOMe)(dppz)](CF_3SO_3)$_3$ 11. Method B, 18 h, 60 °C. Yield 78.1 mg, 70% (Found: C, 38.6; H, 3.5; N, 6.0; S, 10.9. Calc. for $C_{36}H_{36}F_9N_5O_{11}RuS_4$: C, 38.8; H, 3.3; N, 6.3; S, 11.5%). FAB mass spectrum: *m*/*z* 503.9 (100, [(η^6-Mes)-Ru(dppz)]$^+$), 652.9 (75, [(η^6-Mes)Ru(dppz) + $CF_3SO_3]^+$), 815.9 (5, $[M - 2CF_3SO_3]^+$) and 965.9 (20%, $[M - CF_3SO_3]^+$). ^{1}H NMR (CD_3OD): δ 1.72 (s, 3H, δ-CH_3), 2.05 (mm, 4H, β- and γ-CH_2), 2.36 (s, 9H, Mes), 3.77 (s, 3H, CH_3 OMe), 3.98 (br, 1H, α-CH), 6.02 (s, 3H, Mes), 8.19 (dd, 2H), 8.42 (m, 2H), 8.57 (dd, 2H), 9.75 (m, 2H), 10.05 (m, 2H, dppz). ^{13}C NMR (CD_3OD): δ 17.7 (δ-CH_3), 18.9 (Mes), 29.2 (β-CH_2), 34.0 (γ-CH_2), 52.4 (α-CH), 54.3 (CH_3 OMe), 84.0 (Mes), 116.0 (Mes), 129.9, 131.2, 133.0, 134.1, 138.8, 141.0, 144.6, 151.2, 158.0, 158.5 (dppz), 169.7 (COO). $\tilde{\nu}_{max}$/cm^{-1} 1749 (νCO), 1636, 1541 (δNH).

[(η^6-C_6Me_6)Ru(H$_2$metOMe)(dppz)](CF_3SO_3)$_3$ 12. Method B, 18 h, 60 °C. Yield 83.3 mg, 72% (Found: C, 40.1; H, 3.7; N, 6.0. Calc. for $C_{39}H_{42}F_9N_5O_{11}RuS_4$: C, 40.5; H, 3.7; N, 6.1%). FAB mass spectrum: *m*/*z* 546.1 (80, [(η^6-C_6Me_6)Ru(dppz)]$^+$), 695.1 (100, [(η^6-C_6Me_6)Ru(dppz) + $CF_3SO_3]^+$), 858.1 (3, $[M - 2CF_3SO_3]^+$) and 1008.2 (10%, $[M - CF_3SO_3]^+$). ^{1}H NMR (CD_3OD): δ 1.67 (s, 3H, δ-CH_3), 1.95 (mm, 4H, β- and γ-CH_2),

2.3 (s, 18H, C_6Me_6), 3.77 (s, 3H, CH_3 OMe), 4.0 (br, 1H, α-CH), 8.19 (dd, 2H), 8.45 (m, 2H), 8.57 (dd, 2H), 9.46 (m, 2H), 10.05 (m, 2H). ^{13}C NMR (CD_3OD): δ 16.1 (C_6Me_6), 16.4 (δ-CH_3), 29.2 (β-CH_2), 32.9 (γ-CH_2), 52.4 (α-CH), 54.3 (CH_3 OMe), 103.3 (C_6Me_6), 130.0, 131.2, 133.4, 134.0, 138.6, 141.1, 144.6, 150.7, 157.4 (dppz), 169.7 (COO). $\tilde{\nu}_{max}$/cm^{-1} 1749 (νCO), 1636, 1535 (δNH).

[(η^6-C_6Me_6)Ru(HglyglyH$_{-1}$cysOH)(dppz)](CF_3SO_3) 13. Method C, 18 h, 50 °C. Yield 71.5 mg, 77% (Found: C, 48.4; H, 4.2; N, 10.1; S, 7.3. Calc. for $C_{38}H_{40}F_3N_7O_7RuS_2$: C, 49.1; H, 4.3; N, 10.6; S, 6.9%). FAB mass spectrum: *m*/*z* 546.1 (90, [(η^6-C_6Me_6)Ru(dppz)]$^+$), 695.0 (100, [(η^6-C_6Me_6)Ru(dppz) + CF_3SO_3]$^+$) and 780.1 (50%, [M − CF_3SO_3]$^+$). ^{1}H NMR (CD_3OD): δ 1.0, 1.4 (2m, 2H, β-CH_2), 2.18 (s, 18H, C_6Me_6), 3.17 (m, 1H, α-CH), 3.72 (s, 2H, α_{gly}-CH_2), 3.83 (s, 2H, α_{gly}-CH_2), 8.15 (dd, 2H), 8.26 (m, 2H), 8.51 (dd, 2H), 9.26 (m, 2H), 9.82 (m, 2H, dppz). ^{13}C NMR (CD_3OD): δ 15.7 (C_6Me_6), 28.0 (β-CH_2), 41.8, 43.2 (α_{gly}-CH_2), 56.6 (α-CH), 98.9 (C6), 128.9, 129.1, 131.1, 133.8, 136.6, 137.1, 141.4, 144.5, 149.9, 156.9 (dppz), 167.9, 170.7, 173.7 (CO). $\tilde{\nu}_{max}$/cm^{-1} 1670 (νCO), 1537 (δNH).

[(η^6-C_6Me_6)Ru(HcysOMe)(dppz)](CF_3SO_3)$_2$ 14. Method B, 18 h, 45 °C. Yield 62.7 mg, 64% (Found: C, 43.9; H, 3.7; N, 7.0; S, 9.7. Calc. for $C_{36}H_{37}F_6N_5O_8RuS_3$: C, 44.2; H, 3.8; N, 7.2; S, 9.8%). FAB mass spectrum: *m*/*z* 398.0 (100, [M − dppz − 2CF_3SO_3]), 546.0 (60, [(η^6-C_6Me_6)Ru(dppz)]$^+$), 679.9 (20, [M − 2CF_3SO_3]$^+$), 695.0 (35, [(η^6-C_6Me_6)Ru(dppz) + CF_3SO_3]$^+$) and 830.0 (35%, [M − CF_3SO_3]$^+$). ^{1}H NMR (CD_3OD): δ 1.1, 1.3 (2m, 2H, β-CH_2), 2.21 (s, 18H, C_6Me_6), 3.12 (br, 1H, α-CH), 3.42 (s, 3H, CH_3 OMe), 8.18 (dd, 2H), 8.33 (m, 2H), 8.55 (dd, 2H), 9.29 (m, 2H), 9.9 (m, 2H, dppz). ^{13}C NMR (CD_3OD): δ 15.8 (C_6Me_6), 30.4 (β-CH_2), 53.7 (CH_3 OMe), 56.3 (α-CH), 99.3 (C_6Me_6), 129.2, 131.2, 133.8, 134.0, 136.9, 141.3, 144.5, 149.9, 156.7, 157.0 (dppz), 169.3 (COO). $\tilde{\nu}_{max}$/cm^{-1} 1750 (νCO), 1536 (δNH).

[(η^6-C_6Me_6)Ru(HglyglymetOH)(dppz)](CF_3SO_3)$_2$ 15. Method C, 24 h, 50 °C. Yield 68.6 mg, 62% (Found: C, 44.1; H, 4.4; N, 8.8; S, 8.5. Calc. for $C_{41}H_{45}F_6N_7O_{10}RuS_3$: C, 44.5; H, 4.1; N, 8.9; S, 8.7%). FAB mass spectrum: *m*/*z* 546.1 (100, [(η^6-C_6Me_6)Ru(dppz)]$^+$), 695.1 (30, [(η^6-C_6Me_6)Ru(dppz) + CF_3SO_3]$^+$), 808.2 (20, [M − 2CF_3SO_3]$^+$) and 958.2 (5%, [M − CF_3SO_3]$^+$). ^{1}H NMR (CD_3OD): δ 1.59 (s, 3H, δ-CH_3), 1.85 (br, 4H, β- and γ-CH_2), 2.30 (s, 18H, C_6Me_6), 3.75 (s, 2H, α_{gly}-CH_2), 3.78 (s, 2H, α_{gly}-CH_2), 4.11 (t, 1H, α-CH), 8.21 (dd, 2H), 8.45 (m, 2H), 8.57 (dd, 2H), 9.43 (m, 2H), 10.05 (m, 2H, dppz). ^{13}C NMR (CD_3OD): δ 16.0 (δ-CH_3), 16.5 (C_6Me_6), 30.7 (β-CH_2), 32.9 (γ-CH_2), 41.8, 43.2 (α_{gly}-CH_2), 55.2 (α-CH), 103.0 (C_6Me_6), 130.3, 131.1, 133.5, 134.2, 138.9, 141.1, 144.7, 151.2, 157.1 (dppz), 168.1, 170.6, 179.4 (CO). $\tilde{\nu}_{max}$/cm^{-1} 1747, 1670 (νCO), 1542 (δNH).

[(η^6-*p*-cymene)Ru(H_2metOMe)(dppz)](CF_3SO_3)$_3$ 16. Method B, 18 h, 60 °C. Yield 76.8 mg, 68% (Found: C, 39.0; H, 3.2; N, 6.5; S, 10.8. Calc. for $C_{37}H_{38}F_9N_5O_{11}RuS_4$: C, 39.3; H, 3.4; N 6.2; S, 11.4%). FAB mass spectrum: *m*/*z* 518 (100, [(η^6-Cy)Ru(dppz)]$^+$), 667 (88, [(η^6-Cy)Ru(dppz) + CF_3SO_3]$^+$), 831 (58, [M − 2CF_3SO_3]$^+$), 980 (56, [M − CF_3SO_3]$^+$). ^{1}H NMR (CD_3OD): δ 1.07, 1.09 (2d, 6H, CH_3 Cy), 1.62 (s, 3H, δ-CH_3), 2.04 (m, 4H, β- and γ-CH_2), 2.41 (s, 3H, CH_3 Cy), 2.79 (sp, 1H, Cy), 3.78 (s, 3H, OMe), 3.96 (m, 1H, α-CH), 6.42, 6.44, 6.63, 6.64 (4d, 4H, Cy), 8.20 (dd, 2H), 8.44 (m, 2H), 8.57 (dd, 2H), 9.88 (dd, 2H), 10.08 (d, 2H). ^{13}C NMR (CD_3OD): δ 17.4 (δ-CH_3), 18.3, 22.5, 22.6 (Cy), 29.0 (β-CH_2), 32.5 (Cy), 34.1 (γ-CH_2), 52.3 (α-CH), 54.4 (OMe), 89.7, 89.8, 92.2, 110.0, 113.5 (Cy), 130.0, 131.1, 133.4, 134.1, 138.9, 140.8, 144.7, 150.4, 159.7 (dppz), 169.6 (COO). $\tilde{\nu}_{max}$/cm^{-1} 1724, 1623 (νCO), 1526 (δNH).

[([9]aneS$_3$)Ru(H_2metOMe)(dppz)](CF_3SO_3)$_3$ 17. Method A with [H_2MetOMe]CF_3SO_3 and [([9]aneS$_3$)Ru(acetone)(dppz)]-(CF_3SO_3)$_2$, 18 h, 60 °C. Yield 78.7 mg, 67% (Found: C, 33.5; H, 3.4; N, 5.7; S, 18.5. Calc. for $C_{33}H_{36}F_9N_5O_{11}RuS_7$: C, 33.8; H, 3.1; N, 6.0; S, 19.1%). FAB mass spectrum: *m*/*z* 563 (40, [M − H_2metOMe − 3CF_3SO_3]$^+$), 713 (100, [M − H_2metOMe − 2CF_3SO_3]$^+$), 876 (10, [M − 2CF_3SO_3]$^+$), 1026 (5, [M − CF_3SO_3]$^+$). ^{1}H NMR (CD_3OD): δ 1.9–2.2 (mm, 2H, β-CH_2), 1.9 (s, 3H, δ-CH_3), 2.4–2.5 (mm, 2H, γ-CH_2), 2.6–3.4 (mm, 12H, CH_2 [9]aneS$_3$), 3.81 (s, 3H, OMe), 4.0 (dd, 1H, α-CH), 8.19 (dd, 2H), 8.31 (dd, 2H), 8.56 (dd, 2H), 9.49 (m, 2H), 10.02 (m, 2H, dppz). ^{13}C NMR (CD_3OD): 17.3 (δ-CH_3), 29.3 (β-CH_2), 33.7, 33.9, 34.0, 34.1, 35.7, 35.8 (γ-CH_2 and CH_2 [9]aneS$_3$), 52.4 (α-CH), 54.3 (OMe), 129.6, 131.2, 133.1, 134.0, 137.3, 141.2, 144.7, 151.4, 156.9 (dppz), 170.0 (COO). $\tilde{\nu}_{max}$/cm^{-1} 1751, 1624, (νCO), 1540 (δNH).

X-Ray crystallography

Crystal data. 3b $C_{31}H_{28}ClF_3N_4O_4RuS$, M = 730.15, monoclinic, space group $P2_1/c$, a = 8.938(2), b = 9.609(2), c = 35.235(7) Å, β = 95.54(3)°, U = 3012(1) Å^3 (by least-squares refinement on diffractometer angles for 15 automatically centred reflections, λ = 0.71073 Å), T = 293 K, Z = 4, D_c = 1.610 g cm^{-3}, F(000) = 1480. Yellow–brown needle shaped crystals, dimensions: 0.35 × 0.3 × 0.18 mm, μ(Mo-Kα) = 0.738 mm^{-1}.

Data collection and processing. Siemens P4 diffractometer, ω mode with scan speed 2.1–22.6° min^{-1}, graphite-monochromated Mo-Kα radiation; 5284 unique reflections measured ($2.29 \leq 2\theta \leq 25.03°$, $+h$, $+k$, $\pm l$), semi-empirical absorption corrections were applied to the intensity data by use of ψ scans; no significant alterations were observed in the control intensities monitored every 100 reflections.

Structure analysis and refinement. The structure was solved by a combination of direct methods and Fourier difference syntheses and refined by full-matrix least-squares against F^2. Hydrogen atoms were included at calculated positions with isotropic temperature factors. Final reliability indices: R_1 = 0.059 [reflections with $I > 2\sigma(I)$] and 0.114 for all 5284 reflections, wR_2 = 0.159 (all data), S (goodness-of-fit) = 1.020, max., min. Δp = 0.703, −0.868 e Å^{-3}. Structure solution and refinement with SHELX-97.[39] Scattering factors and corrections for anomalous dispersion were taken from ref. 40.

CCDC reference number 183725.

See http://www.rsc.org/suppdata/dt/b2/b203569n/ for crystallographic data in CIF or other electronic format.

Acknowledgements

A. F. thanks the Fonds der Chemischen Industrie and the BMBF for the award of a Ph.D. scholarship.

References

1 B. Nordén, P. Lincoln, B. Åkerman and E. Tuite, *Metal Ions in Biological Systems*, eds. A. Sigel and H. Sigel, Marcel Dekker, New York, 1996, vol. 33, p. 177.
2 K. E. Erkkila, D. T. Odom and J. K. Barton, *Chem. Rev.*, 1999, **99**, 2777.
3 A. E. Friedman, J. Chambron, J. Sauvage, N. J. Turro and J. K. Barton, *J. Am. Chem. Soc.*, 1990, **112**, 4960.
4 C. M. Dupureur and J. K. Barton, *Inorg. Chem.*, 1997, **36**, 33.
5 S. S. David and J. K. Barton, *J. Am. Chem. Soc.*, 1993, **115**, 2984.
6 T. K. Schoch, J. L. Hubbard, C. R. Zoch, G.-B. Yi and M. Sørlie, *Inorg. Chem.*, 1996, **35**, 4383.
7 D. Herebian and W. S. Sheldrick, *J. Chem. Soc., Dalton Trans.*, 2002, 966.
8 J. Sartorius and H.-J. Schneider, *J. Chem. Soc., Perkin Trans. 2*, 1997, 2319.
9 J. Sponer, J. Lesczynski and P. Hobza, *J. Phys. Chem.*, 1996, **100**, 5590.

10 J. Sponer, J. Lesczynski, V. Vetter and P. Hobza, *J. Biomol. Struct. Dyn.*, 1996, **13**, 695.
11 D. L. Carlson, D. H. Huchital, E. J. Mantilla, R. D. Sheardy and W. R. Murphy, Jr., *J. Am. Chem. Soc.*, 1993, **115**, 6424.
12 R. B. Nair, E. S. Teng, S. L. Kirkland and C. J. Murphy, *Inorg. Chem.*, 1998, **37**, 139.
13 P. K.-L. Fu and C. Turro, *Chem. Commun.*, 2001, 279.
14 W. S. Sheldrick and S. Heeb, *J. Organomet. Chem.*, 1989, **377**, 357.
15 W. S. Sheldrick and S. Heeb, *Inorg. Chim. Acta*, 1990, **168**, 93.
16 W. S. Sheldrick and A. J. Gleichmann, *J. Organomet. Chem.*, 1994, **470**, 183.
17 U. Koelle, *Coord. Chem. Rev.*, 1994, **135**, 623.
18 P. Annen, S. Schildberg and W. S. Sheldrick, *Inorg. Chim. Acta*, 2000, **307**, 115.
19 A. M. Pyle, J. P. Rehmann, R. Meshoyrer, C. V. Kumar, N. J. Turro and J. K. Barton, *J. Am. Chem. Soc.*, 1989, **111**, 3051.
20 M. T. Carter, M. Rodriguez and A. J. Bard, *J. Am. Chem. Soc.*, 1989, **111**, 8901.
21 S. R. Smith, G. A. Neyhart, W. A. Karlsbeck and H. H. Thorp, *New. J. Chem.*, 1994, **18**, 397.
22 I. Haq, P. Lincoln, D. Suh, B. Nordén, B. Z. Chowdry and J. B. Chaires, *J. Am. Chem. Soc.*, 1995, **117**, 4788.
23 S. Moghaddas, P. Hendry, R. J. Geue, C. Chin, A. M. T. Bygott, A. M. Sargeson and N. E. Dixon, *J. Chem. Soc., Dalton Trans.*, 2000, 2085.
24 C. V. Kumar and E. H. Asuncion, *J. Chem. Soc., Chem. Commun.*, 1992, 470.
25 G. A. Neyhart, N. Grover, S. R. Smith, W. A. Kalsbeck, T. A. Fairley, M. Corey and H. H. Thorp, *J. Am. Chem. Soc.*, 1993, **115**, 4423.
26 M. Cusumano and A. Giannetto, *J. Inorg. Biochem.*, 1997, **65**, 137.
27 C. M. Dupureur and J. K. Barton, *J. Am. Chem. Soc.*, 1994, **116**, 10286.
28 I. Greguric, J. R. Aldrich-Wright and J. G. Collins, *J. Am. Chem. Soc.*, 1997, **119**, 3621.
29 J. G. Collins, A. D. Sleeman, J. R. Aldrich-Wright, I. Greguric and T. W. Hambley, *Inorg. Chem.*, 1998, **37**, 3133.
30 R. E. Holmlin, J. A. Yao and J. K. Barton, *Inorg. Chem.*, 1999, **38**, 174.
31 A. Greguric, I. D. Greguric, T. W. Hambley, J. R. Aldrich-Wright and J. G. Collins, *J. Chem. Soc., Dalton Trans.*, 2002, 849.
32 P. Lincoln, A. Broo and B. Nordén, *J. Am. Chem. Soc.*, 1996, **118**, 2644.
33 M. A. Bennett and A. K. Smith, *J. Chem. Soc., Dalton Trans.*, 1974, 233.
34 M. A. Bennett, T.-N. Huang, T. W. Matheson and A. K. Smith, *Inorg. Synth.*, 1980, **10**, 74.
35 J. Madureira, T. M. Santos, B. J. Goodfellow, M. Lucena, J. P. de Jesus, M. G. Santana-Marques, M. G. B. Drew and V. Felix, *J. Chem. Soc., Dalton Trans.*, 2000, 4422.
36 M. Yamada, Y. Tanaka and Y. Yoshimoto, *Bull. Chem. Soc. Jpn.*, 1992, **65**, 1006.
37 H.-Q. Liu, T. C. Cheng, S.-M. Peng and C.-M. Che, *J. Chem. Soc., Chem. Commun.*, 1995, 1787.
38 J. Marmur, *J. Mol. Biol.*, 1961, **3**, 208.
39 G. M. Sheldrick, SHELX-97, programs for structure solution and refinement, Göttingen, Germany, 1997.
40 *International Tables for X-Ray Crystallography*, Kynoch Press, Birmingham, 1971, vol. 4.